Surface charge mediated cell-surface interaction on piezoelectric materials

Sylvie Ribeiro[1,2], Christina Puckert[3], Clarisse Ribeiro[1,4,], Andreia C. Gomes[2], Michael J. Higgins[3], Senentxu Lanceros-Méndez[5,6]*

[1]Centro/Departamento de Física, Universidade do Minho, 4710-057 Braga, Portugal.

[2]Centre of Molecular and Environmental Biology (CBMA), Universidade do Minho, Campus de Gualtar, 4710-057 Braga, Portugal.

[3]ARC Centre for Electromaterials Science (ACES), Innovation Campus, University of Wollongong, Squires Way, Wollongong, NSW 2500, Australia

[4]CEB - Centre of Biological Engineering, Universidade do Minho, Campus of Gualtar, 4710 057 Braga, Portugal.

[5]BCMaterials, Basque Centre for Materials, Applications and Nanostructures, UPV/EHU Science Park, 48940 Leioa, Spain

[6]IKERBASQUE, Basque Foundation for Science, 48013 Bilbao, Spain.

*Corresponding author: cribeiro@fisica.uminho.pt

KEYWORDS: Piezoelectric materials, Muscle cells, Single Cell Force Spectroscopy, Electrostatic interactions, Cell adhesion, Cell-material interactions

Abstract

Cell-material interactions play an essential role in the development of scaffold-based tissue engineering strategies. Cell therapies are still limited in treating injuries when severe damage causes irreversible loss of muscle cells. Electroactive biomaterials and, in particular, piezoelectric materials offer new opportunities for skeletal muscle tissue engineering, since these materials have demonstrated suitable electroactive microenvironments for tissue development. In this study, the influence of the surface charge of piezoelectric poly(vinylidene fluoride) (PVDF) on cell adhesion was investigated. The cytoskeletal organization of C2C12 myoblast cells grown on different PVDF samples was studied by immunofluorescence staining and the interactions between single live cells and PVDF were analyzed using an Atomic Force Microscopy (AFM) technique termed Single Cell Force Spectroscopy (SCFS). It was demonstrated that C2C12 myoblast cells seeded on samples with net surface charge present a more elongated morphology, this effect being dependent on the surface charge but independent of the poling direction (negative or positive surface charge). It was further shown that the cell de-adhesion forces of individual C2C12 cells were higher on PVDF samples with overall negative surface charge (8.92 ± 0.45 nN) compared to those on non-poled substrates (zero overall surface charge) (4.06 ± 0.20 nN). These findings explicitly demonstrate that the polarization/surface charge is an important parameter to determine cell fate, as it affects C2C12 cell adhesion, which in turn will influence cell behavior, namely cell proliferation and differentiation.

1. Introduction

Piezoelectric materials undergoing mechanical deformation generate an overall surface charge variation (direct piezoelectric effect) or expand/contract in the presence of an applied voltage [1]. Piezoelectricity was first reported in 1880 by Jacques and Pierre Curie [2] and since then piezoelectric materials have been used in different areas such as energy harvesting, sensors and actuators, electronics, biotechnology and, more recently, tissue engineering [3-5]. In particular, piezoelectric polymers are attractive for these applications due to them being easily tailored at the nano-, micro- and macroscale, produced at low-temperatures and at relatively low cost, and characterized by their flexibility and light weight [6]. A variety of natural and synthetic piezoelectric polymers with different surface properties, such as surface charge or roughness, have recently emerged as biomaterials for tissue engineering applications [7]. The use of natural polymers is still inferior to their synthetic counterparts due to their poor mechanical and electrical properties, as well as their often-difficult processing (i.e. isolation/extraction and the possibility to produce larger quantities) and their fabrication, which is less straightforward at this stage. As such, the synthetic piezoelectric polymers have been the largest group of biocompatible polymers used for tissue engineering [8], mainly acting as a passive support for cell proliferation and differentiation.

Many of the major functions in cells and organs of the human body are controlled by ionic currents, electric fields, ion flow and voltage gradients produced by ion channels and pumps, which are key regulators of cell proliferation, migration and differentiation [9]. Herein, it has been shown that piezoelectric materials can be relevant for tissue engineering strategies by enabling electrical stimulation via a mechanical stimulus, which is important for a range of tissues like bone, tendons, ligaments, cartilage and muscle [10-11]. It is important to emphasize that skeletal

muscle is not a piezoelectric tissue, such as bone, but critically requires electro-mechanical stimulus to promote tissue growth and development and, for this reason, piezoelectric polymers represent a promising new approach for skeletal muscle tissue engineering [12]. Piezoelectric polymeric biomaterials such as poly(vinylidene fluoride), PVDF, have been shown to have the necessary biocompatibility and deliver electro-mechanical stimulus to specific cell types [13-15]. More specifically, the effect of PVDF surface charge on the proliferation [14] and differentiation [15] of C2C12 myoblast cells has previously been demonstrated (Figure 1). Analysis of the cell differentiation showed that the maturation index of the formed myotubes was higher on electrically poled samples consisting of surface charges in the presence of differentiation medium, with no significant differences between the positively ("poled +") and negatively ("poled –") charged surfaces. C2C12 proliferation on β-PVDF showed that surface charge (of the poled samples) promoted the elongation of the cells after 1 day. In contrast to the morphology, where both polarizations ("poled +" and "poled –") promoted the elongation, it was found that C2C12 proliferation was higher on the "poled –" β-PVDF. To rationalize effects from the physical surface properties, earlier studies have shown that β-PVDF films have a surface roughness of ≈ 42 nm from peak-to-peak, with no differences between the non-poled and poled β-PVDF samples[16]. However, the polarization of the PVDF electroactive crystalline phase was shown to affect the wettability of the films. The non-poled β-PVDF films are more hydrophobic, with a contact angle of 76.8º, whereas the poled β-PVDF films with surface charge has lower contact angles of 31.8º and 51º for "poled +" and "poled –", respectively [17], showing that surface charge and energy play a role in determining the C2C12 proliferation and differentiation.

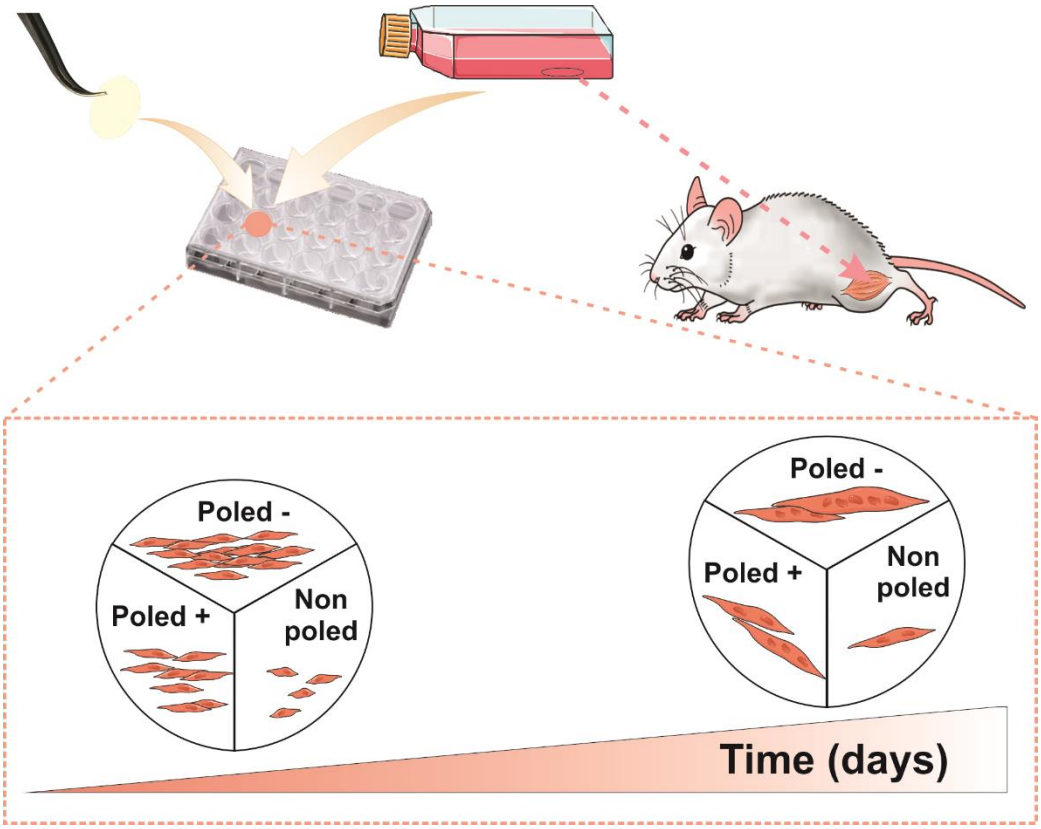

Figure 1 - Schematic representation of the work on C2C12 myoblast proliferation and differentiation on β-PVDF films with different polarization states.

However, the physical interactions and role of cell adhesion, i.e. cell-substrate forces, mediating these effects are not entirely clear, though there is increasing evidence of their relevance in transmitting signals in the development and maintenance of tissues, regulation of cell cycle, migration, differentiation and survival [18]. Three stages characterize the static *in vitro* cell adhesion process: the initial stage is the attachment of the cell body to the material via ligand binding; subsequently, the cell body flattens and spreads due to reorganization of cytoskeletal actin; and lastly, the formation of focal adhesions between cell and the material due to the further actin organization and recruitment of integrins [19]. The more cells that attach and spread on the material's surface, the greater the number of cell adhesive bonds and, therefore, stronger cell

adhesion is expected. Similarly, the adhesion force is related to the number and strength of chemical bonds on the cell surface according to cell adhesion models [19-20]. These dynamic processes of cell adhesion are inextricably linked to changes in cytoskeletal tension and activation of signaling cascades that regulate cell proliferation and differentiation (i.e. gene expression). Most studies to date correlate the material surface properties with cell proliferation and differentiation, which are typically ascertained using conventional staining and fluorescent techniques. Furthermore, the extent of the associated cell adhesion is still often extrapolated from morphological observations such as cells spreading or rounding up, without considering the strength of adhesion [21], or determined using general washing assays by counting the number of cells remaining on the substrate. Therefore, the binding specificity (e.g. type of integrin) and adhesion forces at the cell-material interface are not fully quantified, yet the latest models (e.g. clutch model) show they are critical for transmitting the signals from the material through to the cell's interior [22].

Numerous techniques have been developed to analyze cell adhesion events, including those of single cells [23]. One of these techniques, Single Cell Force Spectroscopy (SCFS), is based on Atomic Force Microscopy (AFM) and represents a versatile approach to quantify single cell adhesion on different substrates, between different cell types, and is showing potential application in mechanobiology [24]. The general idea of SCFS is to replace the tip of the AFM cantilever by a living cell [25]. SCFS offers a large range of detectable forces (e.g. from piconewtons to several nanonewtons), where the measurement of cell detachment enables direct quantification of molecular-level interactions and the forces required to detach a single cell from the substrate. SCFS is a technique more suitable for shorter time studies, i.e. seconds to minutes,

as longer contact times and adhesion to the surface may eventually exceed the binding of the cell to the AFM cantilever.

In this study, we aimed to further understand the effect of piezoelectric β-PVDF (poled samples) surface charge on the C2C12 myoblast cell adhesion. Morphological observations with immunofluorescence staining was used to investigate the cell interactions with two different PVDF surfaces, including those that are "non-poled" (overall zero charge) and "poled" (positive or negative surface charge). In addition, the Atomic Force Microscopy-based technique, Single Cell Force Spectroscopy, was used to provide further insight into the effect of surface charge on the de-adhesion forces and energy required to detach single cells from the PVDF surfaces.

2. Materials and Methods

2.1 Materials

PVDF (Solef 5130, M_W 1,000-1,200 kg/mol) and N,N-dimethylformamide (DMF) were purchased from Solvay and Merck, respectively.

2.2 Preparation of the samples

For the preparation of the PVDF films, the procedure detailed in [6] was applied. A 20% (w/w) solution of PVDF in DMF was prepared under magnetic stirring at room temperature until complete dissolution of the polymer. After that, the solution was spread on a clean glass substrate and heated (J.P. Selecta) at 220 °C for 10 min for solvent evaporation and polymer melting. Then, the samples were cooled at room temperature. After that, the polymer is predominantly in the α-PVDF, so to obtain the piezoelectric phase, β-PVDF, stretching is carried out and films with a thickness around 110 μm were obtained [6, 26]. Sample poling (orientation of

the dipolar moments along the thickness direction of the samples) was achieved by Corona discharge inside a home-made chamber at 10 kV and 10 µA, after an optimization procedure [27]. The measured piezoelectric d_{33} coefficient of the poled samples is ≈ -24 $pC.N^{-1}$. "Non-poled" samples present an overall zero net charge, whereas, once poled, β-PVDF samples can present an overall negative, "poled -", or positive, "poled +", surface charge [16].

The surface free energy (γ_p) values of the PVDF samples were estimated using an adaptation of Young-Dupre equation detailed in [28].

$$\gamma_p = \frac{\gamma_w}{4}(1+\cos\theta)^2 \qquad (1)$$

where θ_0 is the contact angle at equilibrium and γ_w is the water surface energy, (73 mJ m^{-2}).

2.3 Cell Culture

C2C12 myoblast cells (*ATCC*) were cultivated in basal medium (BM) with Dulbecco's Modified Eagle's Medium (DMEM, *Gibco*) with 4.5 $g.L^{-1}$ containing 10% of Fetal Bovine Serum (FBS, *Biochrom*) and 1% of Penicillin/Streptomycin (P/S, *Biochrom).* The cells were grown in 75 cm^2 cell-culture flask at 37 ºC in a humidified air containing 5% CO_2 atmosphere. Every two days, the culture medium was replaced. The cells were detached with 0.05% trypsin-EDTA upon 60-70% confluence. For the AFM measurements and vinculin staining, a suspension of C2C12 with a density of $8x10^4$ $cells.mL^{-1}$ (CO_2-independent media) and $0.8x10^4$ $cells.mL^{-1}$, respectively, was used. For vinculin staining, the suspension of C2C12 was prepared with and without serum for the immunofluorescence assays.

2.4 Immunofluorescence staining

C2C12 cells, with and without protein presence, seeded on different samples were subjected to immunofluorescence staining in order to analyse the presence of focal adhesions contact after 3 h of culture in basal medium. The nucleus, actin and vinculin were stained by 4',6-diamidino-2-phenylindole (DAPI), Tetramethylrhodamine B isothiocyanate (TRITC) and anti-vinculin−FITC antibody (*Sigma-Aldrich*), respectively. At this time, the medium of each well was removed and the cells were washed with PBS 1x and fixed in 4% formaldehyde for 10 minutes at 37 ºC. After this, the samples were again washed with PBS 1x and then incubated with anti-vinculin−FITC antibody (1:50 in PBS 1x) in the dark at room temperature for 1 h. The cells were subsequently counterstained with TRITC (1:200) and DAPI (1µg.mL^{-1}) at room temperature in the dark for 30 and 5 min, respectively. In the end, the samples were rinsed in PBS 1x and after with distilled water, and finally mounted on slides. The samples were visualized using a fluorescence microscope (*Olympus Bx51*) with the appropriate filter sets. The *imageJ* software was used to measure the length and width of the cytoskeleton and also the diameter of the nucleus on all the samples with *feret's* diameter measurement. Experiments were performed on three samples for each condition, and by analyzing ten images for each sample. The graphs were designed in OriginPro 8.5, and Photoshop CS5 was used to assembly the figures for publication. Results were analyzed by Graph Pad Prism Version X for windows (Graph Pad Software, San Diego, CA, U.S.A.). To determine the statistical significances, one-way ANOVA was used. Differences were considered to be significant when $p < 0.05$.

2.5 Single Cell Force Spectroscopy

2.5.1. Cantilever functionalization

The cantilevers were incubated overnight in 50 µL droplets of biotin-BSA solution in a humidified chamber at 37 °C. After that, the cantilevers were washed by immersing and gently moving them in 20 mL of PBS (without Ca^{2+} and Mg^{2+}) filled into a petri dish, performing a total of three washes. The cantilevers were incubated for 30 min in 50 µL droplets of the diluted streptavidin solution in a humidified chamber at room temperature. Thereafter, the cantilevers were washed again three times in 20 mL PBS (without Ca^{2+}/Mg^{2+}), as previously described. To finish the functionalization, the cantilevers were incubated in 50 µL droplets of diluted concanavalin A-biotin solution in a humidified chamber for 30 min at room temperature. After this time, they were washed three times with PBS and stored in a petri dish containing 10 mL PBS (without Ca^{2+} or Mg^{2+}) at 4 °C for at least one week.

2.5.2. Attachment of Single Cell onto AFM Probes

SCFS was performed using a JPK Biowizard II Atomic Force Microscope (JPK, Germany) mounted on a fully automated Nikon inverted optical microscope. The AFM-inverted optical microscope was fully enclosed in a cell incubation system for temperature and humidity control. The PVDF film was placed in the liquid cell and 600 µl of CO_2-independent medium was injected, with heating applied to enable the CO_2-independent media (without proteins) to reach thermal equilibration at 37 °C. The Concanavalin functionalized tipless cantilever was then brought into approximately 50 µm above the PVDF surface. A further 300 µl of CO_2-independent medium containing the C2C12 cells with a concentration of approximately 80,000/ml cells was then injected into the liquid cell and the cells allowed to settle onto the PVDF surface for a period of 5-10 min. Rounded up cells that were yet to adhere were located with the optical microscope and the functionalized AFM probe was positioned over a single cell.

The cell was attached manually to the apex of the cantilever by lowering the stepper motor in 1 μm steps and making contact with the cell until an applied force of 0.5 nN had been reached. After attaching the cell, the cantilever was retracted 50 μm and the optical microscope was used to confirm that the cell was positioned correctly at the end of the cantilever. Afterwards, the single cell was allowed to adhere for 5 min to ensure the strength of cell attachment to the cantilever was greater than to the PVDF surface during the SCFS. According to previous studies, this procedure combined with the use of short cell contact times (e.g. seconds) with the substrate ensured that the cell adhesion to the cantilever was greater than adhesion to the opposing surface [29].

2.5.3. Force Measurements

Force measurements were performed according to modifications of previous methods [30-31]. After attachment of the cell, the live single cell probe was repositioned over a cell-free region of the PVDF surface and force-distance (F-D) curves were performed with a loading force of 500 pN, contact-time of 1 sec and retraction speed of 20 $\mu m.sec^{-1}$ for all experiments. In this study, a 100 μm z-extended travel stage (provided by the JPK Company) was employed to accommodate the longer-range interactions (~ 10-80 μm) between the cell and PVDF sample, which could be significantly greater than the standard z-travel stage (max 15 μm). At least 10 different cells were measured on each PVDF sample (non-poled and "poled -") and up to 20 force-distance, F-D, curves collected for each cell (from 4 different positions on the sample), giving a total of 200 F-D curves per sample for the analysis.

2.5.4. Force-distance curve analysis

Analysis of the F-D curves was performed using the JPK Data Processing software (Version spm-5.1.11), which enabled the quantification of adhesion force, adhesion energy and detachment length. Raw curves were converted into F-D curves using the measured detection sensitivity and cantilever spring constant [32]. Box-whisker plots were plotted using Origin Pro (2015) b9.2.272 and presented as the mean ± standard error of the mean.

3. Results

3.1 Cell adhesion on different β-PVDF materials

In order to determine if there are significant differences in the cytoskeletal organization of C2C12 cells on the different β-PVDF samples, the cells were stained for vinculin (green), a focal adhesion protein, as well as F-actin (red). The fluorescent images obtained are presented in Figure 2. Vinculin is a 117 kDa cytoplasmic protein, a component of the membrane that is associated to the adhesion complexes, as these linker proteins connect the integrins (bound to the extracellular matrix (ECM)) to the actomyosin cytoskeleton [33]. Also, vinculin is a key protein in the regulation of the contractile forces transmission whereby if the vinculin is absent or present, the contractile force generation is reduced or enhanced, respectively [34-35]. As a first approach, a comparison of the density of vinculin-expressing focal adhesions (FAs), cell dimensions (length and width), and cell morphology was made between C2C12 myoblast cells on the different β-PVDF film samples, including the non-poled, “poled +” and “poled –”.

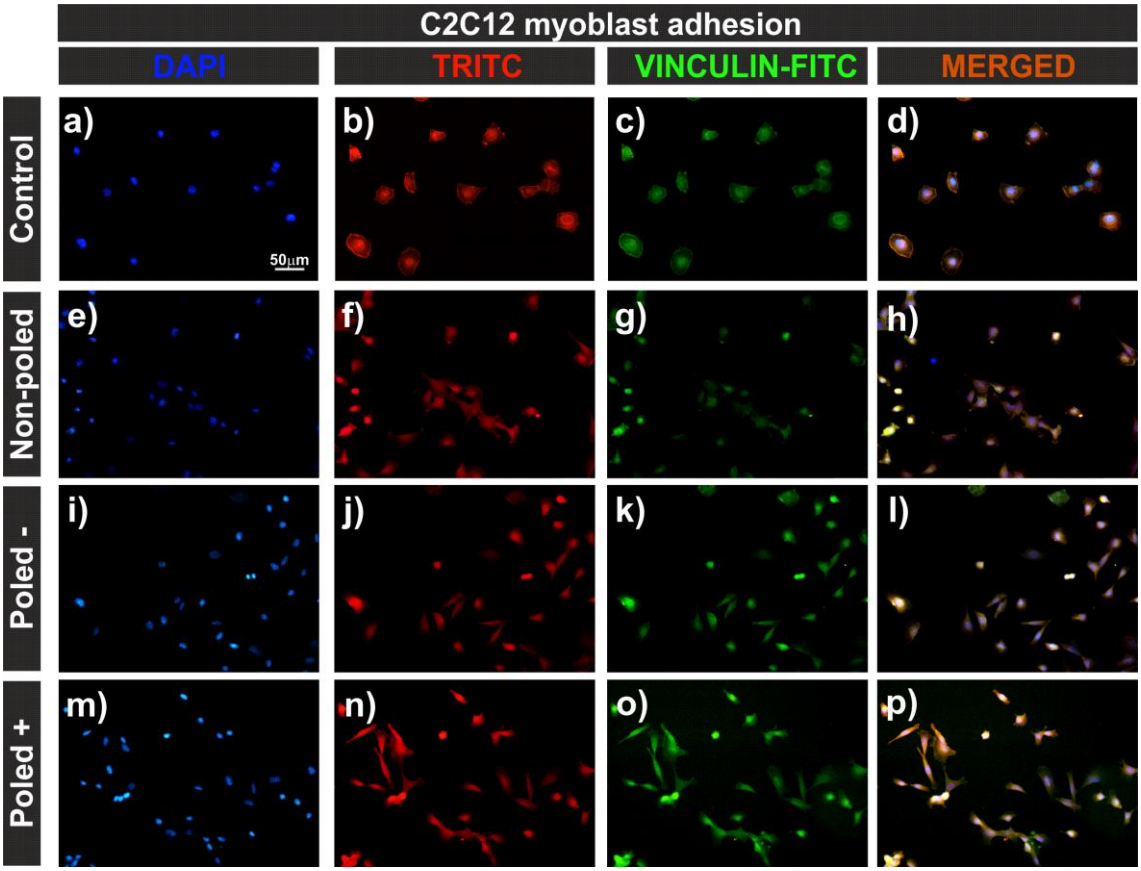

Figure 2 - C2C12 myoblast cells cultured on the surface of polystyrene plate and β-PVDF films after 3h. Fluorescence images of DAPI stained cell nuclei (blue) in a), e), i) and m), vinculin expression (green) in b), f), j) and n), F-actin staining (cytoskeleton, red) in c), g), k) and o), overlay in d), h), l) and p). For comparison cells cultured on polystyrene plate are shown in (a, b, c, d) and those on the different β-PVDF samples are "non-poled" in (e, f, g, h), "poled –" in (i, j, k, l) and "poled +" in (m, n, o, p). The scale bar (50 µm) is valid for all the images.

Immunofluorescence was performed to observe myoblast adhesion and cytoskeletal structure on the different substrates. After 3 h of cell seeding, it was observed that the number of attached cells was similar for all the samples (Figure 2). Moreover, it was observed that C2C12 cells cultured on poled β-PVDF surfaces showed a greater spreading morphology compared with

those on the non-poled β-PVDF and control. In particular, the cell shape on the different substrates were different, especially compared to the control where the cells were distinctly rounded. In addition, staining with vinculin-FITC (green, Figure 2) showed that vinculin was present throughout the cytoplasm of C2C12 cell in all the samples, independently of the sample surface characteristics. In order to quantitatively assess their morphology, the values of length and width of the cytoskeleton, and the nucleus diameter were calculated (Table 1). Table 1 shows that there was an approximately two-fold higher length-to-width ratio on the poled β-PVDF samples, specifically ~ 2.80, compared to 1.33 for non-poled β-PVDF samples, indicating that the cells on the charged surfaces acquired a more elongated morphology. However, there was no significant difference in the cell dimensions, length-to-width ratio, and nucleus size between the differently poled PVDF (Table 1). Hence, these results demonstrate that changes in the C2C12 cell morphology and spreading in response to cell attachment to the PVDF surface was dependent on the existence of surface charge but independent of the polarization state (negative or positive surface charge). It is to notice that the wettability of the samples can have an important role on the cell adhesion, once the poled samples present higher hydrophilicity than the non-poled ones. It is to notice, nevertheless, that in the present case, the wettability of the samples is determined by the surface charge, once surface roughness and surface chemistry are the same, as those issues are not affected by the poling procedure[16]. In this way, the discussion is focused on the surface charge of the samples and its influence on the cell adhesion.

Table 1 - Length and width of the myoblast cells and nucleus diameter after 3 h of incubation in the β-PVDF samples with different surface charges. The values are presented as average ± SD. $^{\#}p \leq 0.0001$ vs Control and $^{*}p \leq 0.0001$ vs Non-poled for each parameter.

Samples	Length (µm)	Width (µm)	Length/width	Nucleus diameter (µm)
Control	27.91 ± 4.88	22.84 ± 4.77	1.27 ± 0.21	10.73 ± 1.44
Non-poled	30.81 ± 7.16 #	23.42 ± 5.13	1.33 ± 0.27	10.24 ± 1.34
Poled +	41.02 ± 8.50 # *	15.33 ± 3.75 # *	2.81 ± 0.30	8.29 ± 1.39 # *
Poled -	40.91 ± 6.47 # *	15.79 ± 2.56 # *	2.80 ± 0.33	8.26 ± 1.73 # *

Figure 3 demonstrates the focal adhesions and the morphology of the C2C12 myoblast cells cultured on the β-PVDF samples. The higher resolution images of single cells after 3 h confirm that C2C12 myoblast cells cultured on poled samples are more elongated than those cultured on non-poled samples (figure 3), in agreement with the literature [14]. Further, relative to the control sample, it seems that the vinculin expression and intensity are higher on all PVDF samples, forming a ring around the nucleus and smaller regions around the edge of the cell. There are no significative differences between the samples with and without proteins.

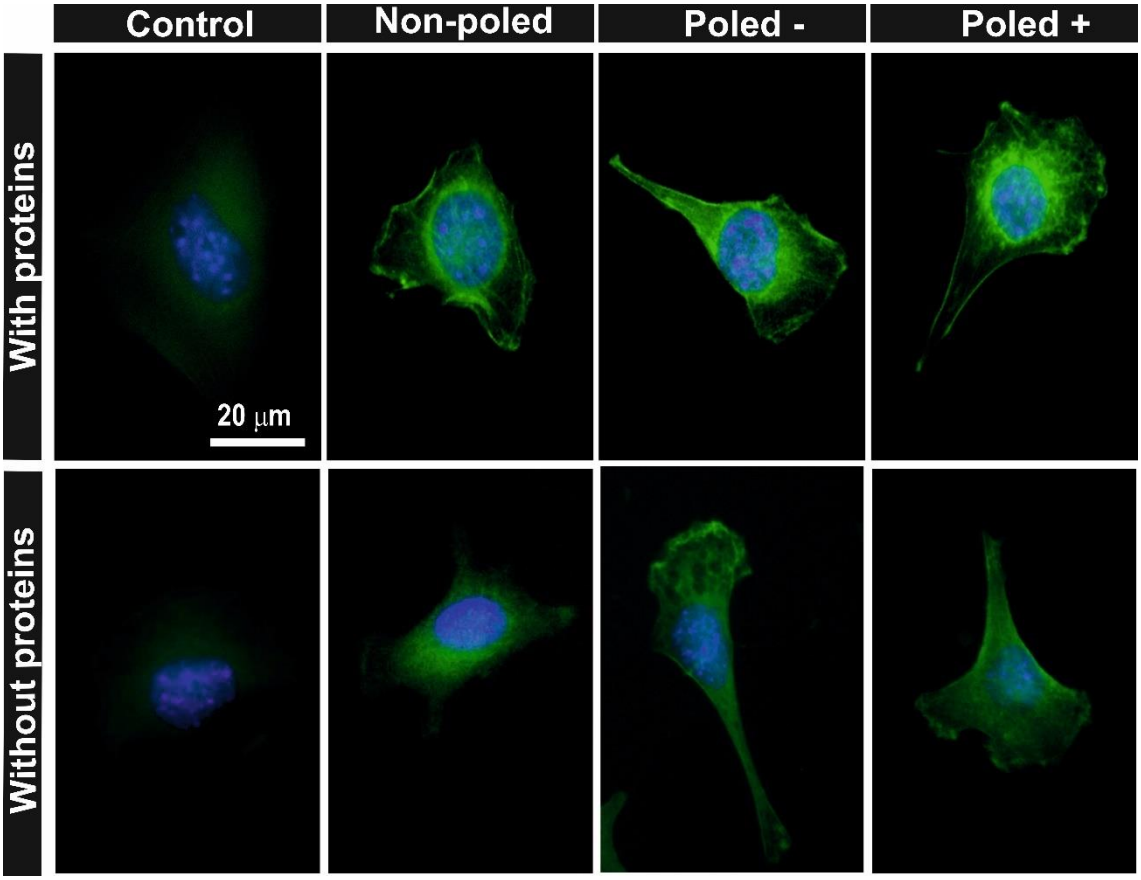

Figure 3 - Immunofluorescence to analyze de focal adhesion by anti-vinculin FITC antibody staining of the C2C12 myoblast cells cultured 3 h on the control and β-PVDF samples ("non-poled", "poled -" and "poled +") with and without proteins. The scale bar of 20 μm is valid for all the images.

3.2 Single Cell Force Spectroscopy

As mentioned, poled β-PVDF was previously shown to promote the elongation of C2C12 myoblasts [14], which is in agreement with our observations in Figure 2 and 3, and the length-to-width ratio values in Table 1. In the same study, the "poled –" β-PVDF, (negatively charged surface) enhanced the C2C12 proliferation (after 3 days) compared to the "non-poled" and "poled +" β-PVDF samples [14]. Given that the cell adhesion is an important process underlying

these different cell responses [36], we attempt to evaluate the adhesion forces measured by SCFS. To this end, this SCFS initial investigation was used to directly probe the ability of the PVDF support the initial C2C12 myoblast cell adhesion without proteins. For that, the negatively charged (poled -) β-PVDF film versus the non-charged - zero average charge - (non-poled) β-PVDF film were selected in order to study the influence of a charged surface relative to a non-charged surface (non-poled sample). More specifically, the negatively charged surface was a focus as these surfaces enhanced the cell proliferation and differentiation [11]. For the SCFS experiments, a single C2C12 cell was attached to a functionalized cantilever (Figure 4a). The attached cell was then lowered to the β-PVDF substrate (Figure 4b) until a pre-set force was reached. After a contact time of 1-3 sec to allow the formation of adhesive interactions, the cantilever was retracted until the cell and substrate were completely separated (Figure 4c). During the approach and retraction of the cantilever, the force versus distance (F-D) curves were obtained and analysed.

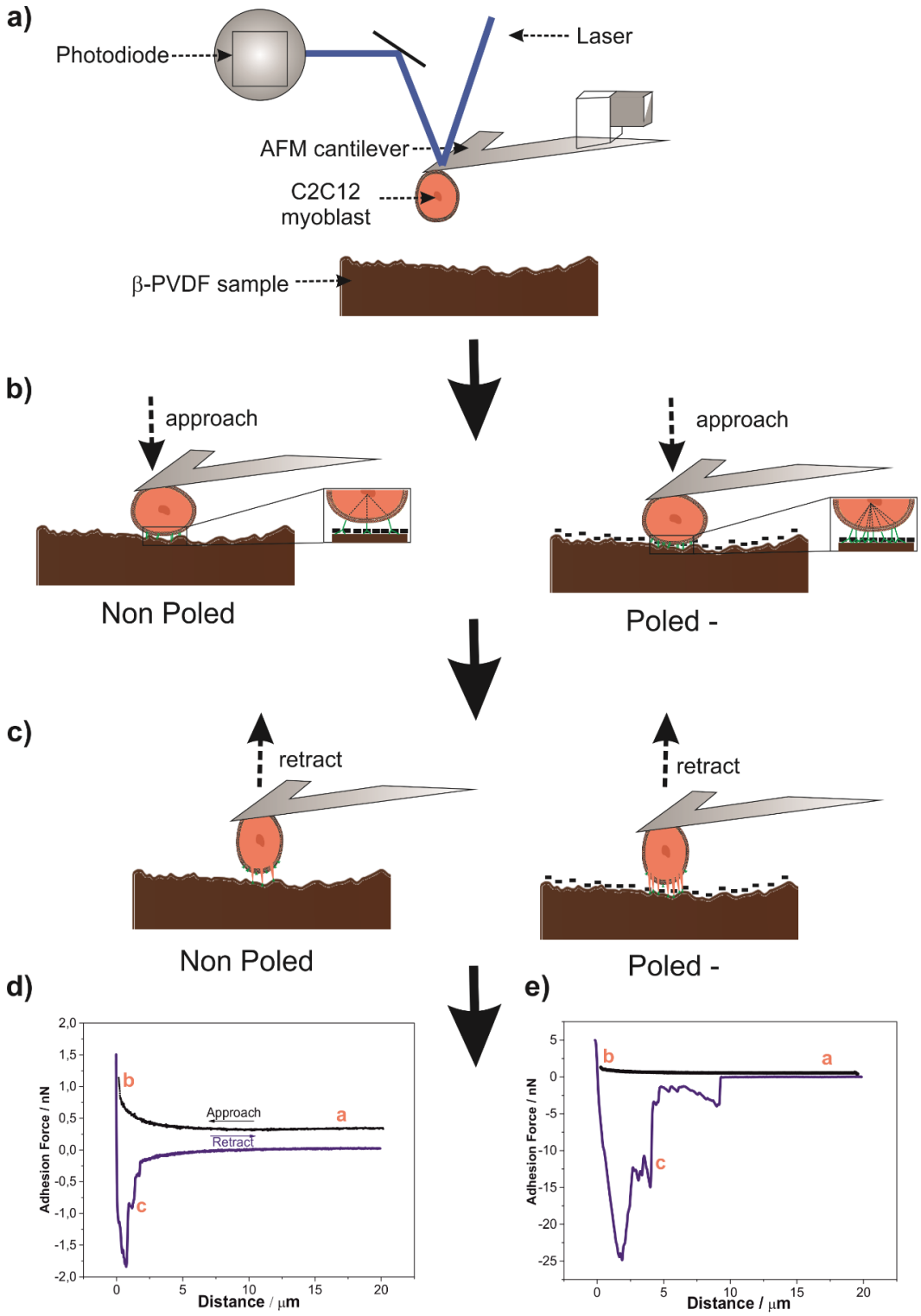

Figure 4 - Single cell force spectroscopy. a) All the elements involved in the test and the AFM cantilever are positioned above the cell after the cantilever functionalization. b) The cantilever-bound cell is lowered towards on the polymer support until a pre-set force is reached. c) After a

given preset contact time, the cantilever is retracted until cell and substrate are completely separated. Representative Force-Distance curves recorded while repeatedly detaching a single C2C12 myoblast cell from β-PVDF samples with different surface charges: d) “Non-poled” and e) “Poled -”.

Figure 4d and 4e show the F-D curves for “non-poled” and “poled -” β-PVDF obtained by SCFS, respectively. The F-D curves show that C2C12 myoblast cells on the negative poled β-PVDF present significantly higher peak forces in the retraction curves (figure 4e) compared to those on the non-poled β-PVDF (figure 4d). Here, the peak maximum represents a measure of the bulk single cell de-adhesion [24] although the presence of subsequent peaks indicates the sequential detachment of fewer, remaining adhesive bonds. Thus, the F-D curves confirmed that higher de-adhesion forces occurred on the negatively charged β-PVDF surfaces, presumably due to stronger electrostatic interactions between the PVDF and charged cell surface molecules (non-specific interaction) and also given that there are no proteins present in the medium. The larger magnitude of cell de-adhesion on the negatively charged β-PVDF surfaces was also evident by the presence of several larger peaks in Figure 4e, in addition to the greater de-adhesion energy that is given by the integrated area under the retraction curve. From analysis of the F-D curves, the maximum de-adhesion force (maximum peak force), de-adhesion energy (integrated area under the F-D curve) and the distance required to completely detach the cell from the surface are shown in Figure 5.

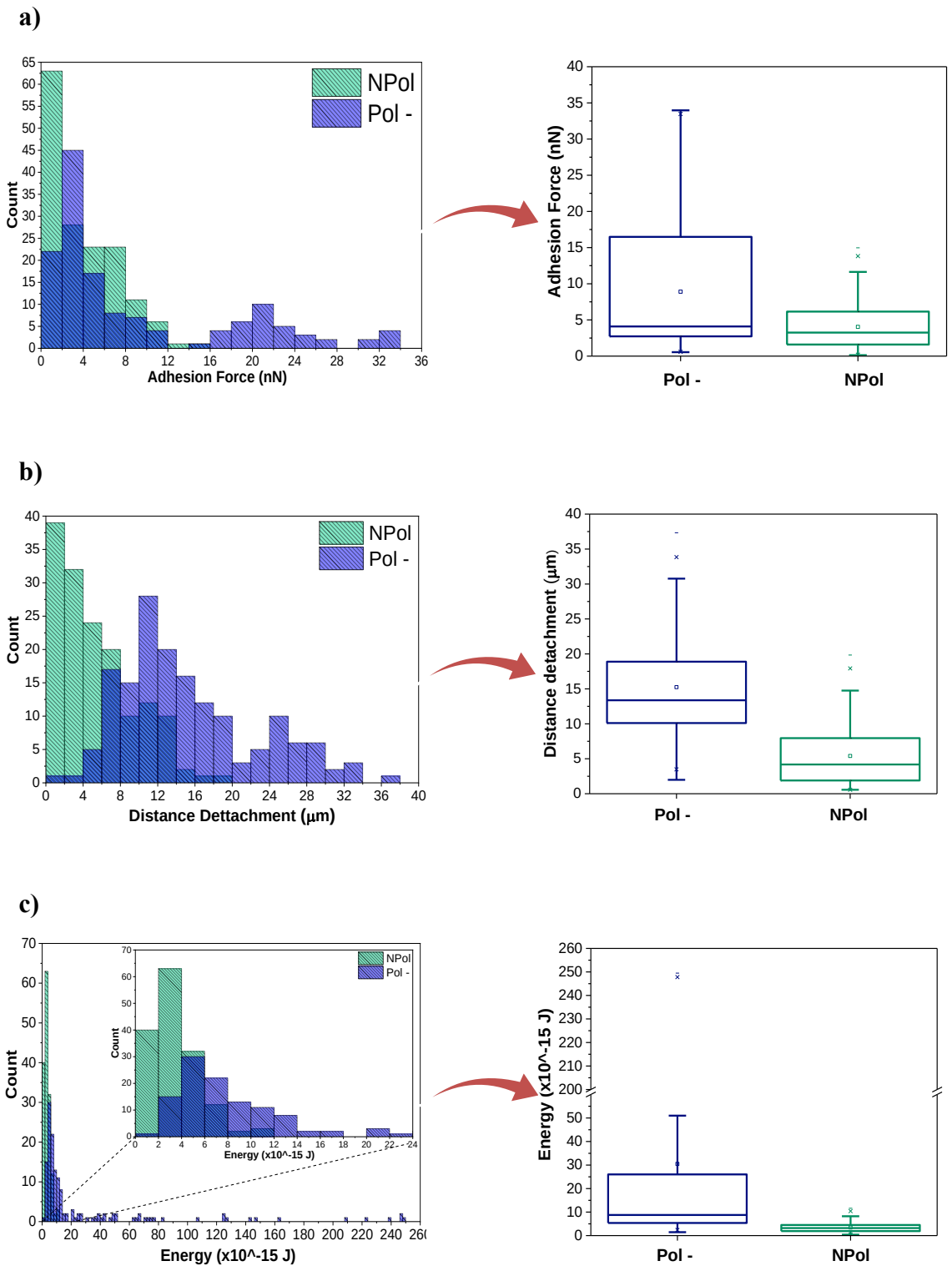

Figure 5 - Comparison of histograms for the a) maximum de-adhesion force, b) distance detachment and c) adhesion energy.

Whisker plots verified that the de-adhesion force of individual C2C12 cells was higher on “poled –” β-PVDF samples (8.92 ± 0.45 nN) than on non-poled substrates (4.06 ± 0.20 nN) (Figure 5a). The higher de-adhesion force value of “poled –” β-PVDF was associated with an increase in de-adhesion energy (30.34 ± 1.52 × 10^{-15} J) and detachment distance (15.28 ± 0.76 μm) of the C2C12 myoblast cell compared to the non-poled surface (3.38 ± 0.17 × 10^{-15} J and 5.27 ± 0.26 μm), respectively (Figure 5c and b). Furthermore, histograms of de-adhesion force (Figure 5a) and distance detachment (Figure 5b) revealed that the "poled -" β-PVDF samples consisted to two peak distribution, but this was not observed for the de-adhesion energy (Figure 5c). The peak values of these distributions were 4 ± 0.2 nN and 22 ± 1.1 nN for the de-adhesion force, and 12 ± 0.6 μm and 26 ± 1.3 μm for distance detachment. In contrast, the non-poled β-PVDF samples showed only a single distribution, with the appearance of a half-normal distribution for de-adhesion force (Figure 5a) and distance detachment (Figure 5b). Specifically, the distribution for de-adhesion forces overlapped with the lower peak distribution of the "poled -" β-PVDF samples (Figure 5a) though for the detachment distance the non-poled β-PVDF distribution was lower than both distributions of the "poled -" β-PVDF samples (Figure 5b).

4. Discussion/Conclusion

In this study, two different approaches were performed to distinguish the effect of PVDF material properties on the cell response, firstly via immunofluorescence staining of cells after 3 h in serum-containing media to elucidate the surface charge effects on the cell morphology and focal adhesion - vinculin. The results demonstrated that the poled (surface charged) PVDF

enhanced cell spreading morphology and greater expression of vinculin compared to the control, suggesting that this cell adhesion promoted by the electrical poling of PVDF is importantly related to previous observations of increased myoblast differentiation and maturation of myotubes on the same surfaces.

Having confirmed the effects from our previous studies, the focus of the study was to then probe the C2C12 cell adhesive interactions on the non-poled versus poled PVDF. This was done using SCFS and on the negatively charged surfaces but in this case under serum-free conditions to investigate purely the initial electrostatic interactions. During the initial adhesion process, electrostatic interactions may also influence the myoblasts, promoting cell adhesion and subsequent responses such as morphology elongation. Thus, as a first step to elucidate the different cell adhesion mechanisms, such as electrostatic interaction, hydrophobic interaction, and biological interaction [37], the SCFS was performed in the aforementioned serum-free media.

It has been commonly assumed that positively charged substrates promote cell adhesion through electrostatic interaction, e.g. through use of positively charged poly-l-lysine on cell culture substrates, with the negative charge of the cell membrane, while negatively charged substrates would be expected to suppress cell adhesion. However, previous studies demonstrate that cells adhere to both positively and negatively charged surfaces, even within short periods of incubation [37]. Also, the influence of gold nanoparticles positively- and negatively-charged groups on their internalization by HOB cells was investigated and it has been shown that different surface charges can be internalized, irrespective of the presence or absence of serum proteins in the media [38]. The surface charge density can also improve the penetration efficiency [39]. In this case, the wettability of the samples was calculated by measuring the WCA and the values confirm the results from the literature: 76.8º for non-poled and 51º for “poled –” samples.

With those values and equation 1, the surface free energy was calculated, the non-poled samples presenting a value of 27.5 $mJ.m^{-2}$ and the "poled –" β-PVDF samples a value of 48.5 $mJ.m^{-2}$. In this study, the SCFS directly verified that single C2C12 cells could adhere strongly to negatively charged surfaces without adsorbed proteins within contact times of seconds. In contrast, de-adhesion forces comprising significantly fewer interactions occurring over much smaller distances, presumably also responsible for the reduced de-adhesion energy, were observed on the non-poled (non-charged). These findings are in agreement with a previous study of *Hoshiba* and co-authors, where it was demonstrated that the cell adhesion force was higher on charged surfaces, it is independent of the proteins presence or absence [37].

The box-whisker plots showed clear differences in the cells de-adhesion, however, the histogram analysis revealed a more complex response of the cell de-adhesion. For instance, two peak distributions (blue peaks) were observed for the negatively poled surface, suggesting that the surface charge distribution of the "poled –" β-PVDF is not homogeneous due to the semicrystalline nature of the polymer [40], leading to some regions where the cell can form stronger adhesion and less adhesion in other regions. In particular, the peak values of ~ 20-25 nN in the higher distribution, are remarkably high for the single cell de-adhesion in comparison to those measured in other SCFS studies where the single cell forces are typically < 1 nN [41]. We suggest that the high de-adhesion values may be related to either the high charge density of electroactive PVDF [1] and/or possible effects from the approach and contact of the cantilever with the PVDF surface that generates a mechanical stimulus, which in turn induces electrical polarization of the PVDF.

In conclusion, the molecular interactions between C2C12 myoblast cell and piezoelectric polymer films, β-PVDF, with different surface charges, positive, negative or neutral, were

analysed with the AFM-based SCFS technique and immunofluorescence tests. It was demonstrated that surface charge promotes cell elongation and negative polarization improves cell-material adhesion. The de-adhesion energy required to detach the cell is higher on negative charged surfaces, which is concomitant with higher de-adhesion force exerted on the cantilever. This study is the first in vitro study to directly quantify the adhesive forces of cells on PVDF, including the effect of negative polarization state and surface charge of piezoelectric β-PVDF films on C2C12 cells. β-PVDF with polarization offers potential for skeletal muscle tissue engineering applications, allowing one to tune cell-surface interactions via electrical poling and also dynamically from the piezoelectric effect.

A key issue is that the SCFS reveals a distinct difference in cell interaction (forces, energy) for poled versus non-poled samples which in turn affects the cell behaviour with respect to the cell adhesion. This fact is evidenced by the results obtained from the morphological and fluorescence observations (figure 2), where cells cultured on charged surfaces present an more elongated morphology, in agreement with previous studies showing that charged surfaces promote an earlier formation of myocytes, which are necessary for differentiation of myoblasts into myotubes, and consequently skeletal muscle tissue [12]. Through physical attachment to actin filaments within the cellular network, focal adhesions allow cells to pull or push themselves along a matrix during migration. The substrate properties such as stiffness, topography and surface energy/charge are important parameters determining the resistance of the substrate to deformation by cell traction forces, which enable cells to travel with persistent direction [42]. Molecular pathways underlying cell proliferation are also regulated via contractile forces imparted by the actin network and sensed by focal adhesions.

Regarding cell morphological observations and forces measured by SCFS, it is proposed that cell spreading and elongation correlates with larger adhesion to the charged surface. The increased tensile forces (i.e. the forces the cell feels when it “pulls” on the surface otherwise known as traction forces) activate actin expression/reorganization, enabling cells to increase its area on the substrate. From the SCFS, the charged groups of "poled -" β-PVDF surface act as “ligands” based on electrostatic forces with charged cell membrane molecules, resulting in stronger adhesion forces. Thus, this will enable the cells to spread and elongate.

ACKNOWLEDGMENT

This work was supported by the Portuguese Foundation for Science and Technology (FCT) in the framework of the Strategic Funding UID/FIS/04650/2019, UID/BIA/04050/2013, UID/BIO/04469, project POCI-01-0145-FEDER-028237 and under BioTecNorte operation (NORTE-01-0145-FEDER-000004). The authors also thank the FCT for the SFRH/BD/111478/2015 (S.R.) and SFRH/BPD/90870/2012 (C.R.) grants. Funds provided by FCT in the framework of EuroNanoMed 2016 call, Project LungChek ENMed/0049/2016 are also gratefully acknowledged. The authors acknowledge funding by the Spanish Ministry of Economy and Competitiveness (MINECO) through the project MAT2016-76039-C4-3-R (AEI/FEDER, UE) and from the Basque Government Industry and Education Department under the ELKARTEK, HAZITEK and PIBA (PIBA-2018-06) programs, respectively.

REFERENCES

(1) Martins, P.; Lopes, A. C.; Lanceros-Mendez, S. Electroactive Phases of Poly(vinylidene fluoride): Determination, Processing and Applications. *Progress in Polymer Science* **2014,** *39* (4), 683-706, DOI: 10.1016/j.progpolymsci.2013.07.006.

(2) Mould, R. F. Marie and Pierre Curie and radium: History, Mystery, and Discovery. *Medical Physics* **1999,** *26* (9), 1766-1772, DOI: 10.1118/1.598680.

(3) Usher, T. D.; Cousins, K. R.; Zhang, R.; Ducharme, S. The Promise of Piezoelectric Polymers. *Polymer International* **2018,** *67* (7), 790-798, DOI: 10.1002/pi.5584.

(4) Zhang, Y.; An, Q.; Tong, W.; Li, H.; Ma, Z.; Zhou, Y.; Huang, T. A New Way to Promote Molecular Drug Release during Medical Treatment: A Polyelectrolyte Matrix on a Piezoelectric–Dielectric Energy Conversion Substrate. *Small* **2018,** *14* (37), DOI: 10.1002/smll.201802136.

(5) Hu, F.; Cai, Q.; Liao, F.; Shao, M.; Lee, S. T. Recent Advancements in Nanogenerators for Energy Harvesting. *Small* **2015,** *11* (42), 5611-5628, DOI: 10.1002/smll.201501011.

(6) Ribeiro, C.; Costa, C. M.; Correia, D. M.; Nunes-Pereira, J.; Oliveira, J.; Martins, P.; Gonçalves, R.; Cardoso, V. F.; Lanceros-Méndez, S. Electroactive Poly(vinylidene fluoride)-based Structures for Advanced Applications. *Nature Protocols* **2018,** *13* (4), 681-704, DOI: 10.1038/nprot.2017.157.

(7) Dhandayuthapani, B.; Yoshida, Y.; Maekawa, T.; Kumar, D. S. Polymeric Scaffolds in Tissue Engineering Application: A Review. *International Journal of Polymer Science* **2011,** *2011*, DOI: 10.1155/2011/290602.

(8) Guo, B.; Ma, P. X. Synthetic Biodegradable Functional Polymers for Tissue Engineering: A Brief Review. *Science China Chemistry* **2014,** *57* (4), 490-500, DOI: 10.1007/s11426-014-5086-y.

(9) Levin, M. Molecular Bioelectricity in Developmental Biology: New Tools and Recent Discoveries: Control of Cell Behavior and Pattern Formation by Transmembrane Potential Gradients. *BioEssays* **2012,** *34* (3), 205-217, DOI: 10.1002/bies.201100136.

(10) Ribeiro, C.; Sencadas, V.; Correia, D. M.; Lanceros-Méndez, S. Piezoelectric Polymers as Biomaterials for Tissue Engineering Applications. *Colloids and Surfaces B: Biointerfaces* **2015,** *136*, 46-55, DOI: 10.1016/j.colsurfb.2015.08.043.

(11) Xiang, H.; Chen, Y. Energy-Converting Nanomedicine. *Small* **2019,** *15* (13), DOI: 10.1002/smll.201805339.

(12) Bach, A. D.; Beier, J. P.; Stern-Staeter, J.; Horch, R. E. Skeletal Muscle Tissue Engineering. *Journal of Cellular and Molecular Medicine* **2004,** *8* (4), 413-422, DOI: 10.1111/j.1582-4934.2004.tb00466.x.

(13) Ribeiro, C.; Pärssinen, J.; Sencadas, V.; Correia, V.; Miettinen, S.; Hytönen, V. P.; Lanceros-Méndez, S. Dynamic Piezoelectric Stimulation Enhances Osteogenic Differentiation of Human Adipose Stem Cells. *Journal of Biomedical Materials Research - Part A* **2015,** *103* (6), 2172-2175, DOI: 10.1002/jbm.a.35368.

(14) Martins, P. M.; Ribeiro, S.; Ribeiro, C.; Sencadas, V.; Gomes, A. C.; Gama, F. M.; Lanceros-Méndez, S. Effect of Poling State and Morphology of Piezoelectric Poly(Vinylidene Fluoride) Membranes for Skeletal Muscle Tissue Engineering. *RSC Advances* **2013,** *3* (39), 17938-17944, DOI: 10.1039/c3ra43499k.

(15) Ribeiro, S.; Gomes, A. C.; Etxebarria, I.; Lanceros-Méndez, S.; Ribeiro, C. Electroactive Biomaterial Surface Engineering Effects on Muscle Cells Differentiation. *Materials Science and Engineering C* **2018,** *92*, 868-874, DOI: 10.1016/j.msec.2018.07.044.

(16) Serrado Nunes, J.; Wu, A.; Gomes, J.; Sencadas, V.; Vilarinho, P. M.; Lanceros-Méndez, S. Relationship Between the Microstructure and the Microscopic Piezoelectric Response of the

α- and β-Phases of Poly(Vinylidene Fluoride). *Applied Physics A: Materials Science and Processing* **2009,** *95* (3), 875-880, DOI: 10.1007/s00339-009-5089-2.

(17) Parssinen, J.; Hammarén, H.; Rahikainen, R.; Sencadas, V.; Ribeiro, C.; Vanhatupa, S.; Miettinen, S.; Lanceros-Méndez, S.; Hytönen, V. P. Enhancement of Adhesion and Promotion of Osteogenic Differentiation of Human Adipose Stem Cells by Poled Electroactive Poly(Vinylidene Fluoride). *Journal of Biomedical Materials Research - Part A* **2015,** *103* (3), 919-928, DOI: 10.1002/jbm.a.35234.

(18) Huang, S.; Ingber, D. E. The Structural and Mechanical Complexity of Cell-Growth Control. *Nature Cell Biology* **1999,** *1* (5), E131-E138, DOI: 10.1038/13043.

(19) Khalili, A. A.; Ahmad, M. R. A Review of Cell Adhesion Studies for Biomedical and Biological Applications. *International Journal of Molecular Sciences* **2015,** *16* (8), 18149-18184, DOI: 10.3390/ijms160818149.

(20) Dembo, M.; Torney, D. C.; Saxman, K.; Hammer, D. The Reaction-Limited Kinetics of Membrane-to-Surface Adhesion and Detachment. *Proceedings of the Royal Society B: Biological Sciences* **1988,** *234* (1274), 55-83, DOI: 10.1098/rspb.1988.0038.

(21) Resende, R. R.; Fonseca, E. A.; Tonelli, F. M. P.; Sousa, B. R.; Santos, A. K.; Gomes, K. N.; Guatimosim, S.; Kihara, A. H.; Ladeira, L. O. Scale/Topography of Substrates Surface Resembling Extracellular Matrix for Tissue Engineering. *Journal of Biomedical Nanotechnology* **2014,** *10* (7), 1157-1193, DOI: 10.1166/jbn.2014.1850.

(22) Sun, Z.; Guo, S. S.; Fässler, R. Integrin-Mediated Mechanotransduction. *Journal of Cell Biology* **2016,** *215* (4), 445-456, DOI: 10.1083/jcb.201609037.

(23) Friedrichs, J.; Legate, K. R.; Schubert, R.; Bharadwaj, M.; Werner, C.; Müller, D. J.; Benoit, M. A Practical Guide to Quantify Cell Adhesion Using Single-Cell Force Spectroscopy. *Methods* **2013,** *60* (2), 169-178, DOI: 10.1016/j.ymeth.2013.01.006.

(24) Yu, M.; Strohmeyer, N.; Wang, J.; Müller, D. J.; Helenius, J. Increasing Throughput of AFM-based Single Cell Adhesion Measurements through Multisubstrate Surfaces. *Beilstein Journal of Nanotechnology* **2015,** *6* (1), 157-166, DOI: 10.3762/bjnano.6.15.

(25) Beaussart, A.; El-Kirat-Chatel, S.; Herman, P.; Alsteens, D.; Mahillon, J.; Hols, P.; Dufrêne, Y. F. Single-Cell Force Spectroscopy of Probiotic Bacteria. *Biophysical Journal* **2013,** *104* (9), 1886-1892, DOI: 10.1016/j.bpj.2013.03.046.

(26) Sencadas, V.; Gregorio, R.; Lanceros-Mendez, S. Alpha to Beta Phase Transformation and Microestructural Changes of PVDF Films Induced by Uniaxial Stretch. *Journal of Macromolecular Science Part B-Physics* **2009,** *48* (3), 514-525, DOI: 10.1080/00222340902837527.

(27) Cardoso, V. F.; Minas, G.; Lanceros-Mendez, S. Multi Layer Spin-Coating Deposition of Poly(Vinylidene Fluoride) Films for Controlling Thickness and Piezoelectric Response. *Sensors and Actuators a-Physical* **2013,** *192*, 76-80, DOI: 10.1016/j.sna.2012.12.019.

(28) Martins, P. M.; Miranda, R.; Marques, J.; Tavares, C. J.; Botelho, G.; Lanceros-Mendez, S. Comparative efficiency of TiO_2 nanoparticles in suspension vs. immobilization into P(VDF-TrFE) porous membranes. *RSC Advances* **2016,** *6* (15), 12708-12716, DOI: 10.1039/c5ra25385c.

(29) Wojcikiewicz, E. P.; Zhang, X.; Chen, A.; Moy, V. T. Contributions of Molecular Binding Events and Cellular Compliance to the Modulation of Leukocyte Adhesion. *J Cell Sci* **2003,** *116* (Pt 12), 2531-9, DOI: 10.1242/jcs.00465.

(30) Zhang, H.; Molino, P. J.; Wallace, G. G.; Higgins, M. J. Quantifying Molecular-Level Cell Adhesion on Electroactive Conducting Polymers using Electrochemical-Single Cell Force Spectroscopy. *Scientific Reports* **2015,** *5*, 13334, DOI: 10.1038/srep13334.

(31) Zhang, H.; Gu, Q.; Wallace, G. G.; Higgins, M. J. Effect of Electrochemical Oxidation and Reduction on Cell De-Adhesion at the Conducting Polymer–Live Cell Interface as Revealed by Single Cell Force Spectroscopy. *Biointerphases* **2018,** *13* (4), 041004, DOI: 10.1116/1.5022713.

(32) Puckert, C.; Higgins, M. J. Force Spectroscopy. In *Compendium of Surface and Interface Analysis*; The Surface Science Society of, J., Ed.; Springer Singapore: Singapore, 2018; pp 193-200.

(33) Peng, X.; Nelson, E. S.; Maiers, J. L.; DeMali, K. A., New Insights into Vinculin Function and Regulation. In *International Review of Cell and Molecular Biology*, 2011; Vol. 287, pp 191-231.

(34) Mierke, C. T.; Kollmannsberger, P.; Zitterbart, D. P.; Smith, J.; Fabry, B.; Goldmann, W. H. Mechano-Coupling and Regulation of Contractility by the Vinculin Tail Domain. *Biophysical Journal* **2008,** *94* (2), 661-670, DOI: 10.1529/biophysj.107.108472.

(35) Mierke, C. T. The Role of Vinculin in the Regulation of the Mechanical Properties of Cells. *Cell Biochemistry and Biophysics* **2009,** *53* (3), 115-126, DOI: 10.1007/s12013-009-9047-6.

(36) Chang, H. Y.; Kao, W. L.; You, Y. W.; Chu, Y. H.; Chu, K. J.; Chen, P. J.; Wu, C. Y.; Lee, Y. H.; Shyue, J. J. Effect of Surface Potential on Epithelial Cell Adhesion, Proliferation and Morphology. *Colloids and Surfaces B: Biointerfaces* **2016,** *141*, 179-186, DOI: 10.1016/j.colsurfb.2016.01.049.

(37) Hoshiba, T.; Yoshikawa, C.; Sakakibara, K. Characterization of Initial Cell Adhesion on Charged Polymer Substrates in Serum-Containing and Serum-Free Media. *Langmuir* **2018,** *34* (13), 4043-4051, DOI: 10.1021/acs.langmuir.8b00233.

(38) Allen, C.; Qiu, T. A.; Pramanik, S.; Buchman, J. T.; Krause, M. O. P.; Murphy, C. J. Research Highlights: Investigating the Role of Nanoparticle Surface Charge in Nano-Bio Interactions. *Environmental Science: Nano* **2017,** *4* (4), 741-746, DOI: 10.1039/c7en90014g.

(39) Quan, X.; Peng, C.; Zhao, D.; Li, L.; Fan, J.; Zhou, J. Molecular Understanding of the Penetration of Functionalized Gold Nanoparticles into Asymmetric Membranes. *Langmuir* **2017,** *33* (1), 361-371, DOI: 10.1021/acs.langmuir.6b02937.

(40) Ribeiro, C.; Moreira, S.; Correia, V.; Sencadas, V.; Rocha, J. G.; Gama, F. M.; Gómez Ribelles, J. L.; Lanceros-Méndez, S. Enhanced Proliferation of Pre-Osteoblastic Cells by Dynamic Piezoelectric Stimulation. *RSC Advances* **2012,** *2* (30), 11504-11509, DOI: 10.1039/c2ra21841k.

(41) Helenius, J.; Heisenberg, C. P.; Gaub, H. E.; Muller, D. J. Single-Cell Force Spectroscopy. *Journal of Cell Science* **2008,** *121* (11), 1785-1791, DOI: 10.1242/jcs.030999.

(42) Kennedy, K. M.; Bhaw-Luximon, A.; Jhurry, D. Cell-Matrix Mechanical Interaction in Electrospun Polymeric Scaffolds for Tissue Engineering: Implications for Scaffold Design and Performance. *Acta Biomaterialia* **2017,** *50*, 41-55, DOI: 10.1016/j.actbio.2016.12.034.

Graphic for manuscript